

M. Kempenaars, J.C. Flanagan, L. Giudicotti, M.J. Walsh, M. Beurskens,
I. Balboa and JET EFDA contributors

Enhancement of the JET Edge LIDAR Thomson Scattering Diagnostic with Ultra Fast Detectors

"This document is intended for publication in the open literature. It is made available on the understanding that it may not be further circulated and extracts or references may not be published prior to publication of the original when applicable, or without the consent of the Publications Officer, EFDA, Culham Science Centre, Abingdon, Oxon, OX14 3DB, UK."

"Enquiries about Copyright and reproduction should be addressed to the Publications Officer, EFDA, Culham Science Centre, Abingdon, Oxon, OX14 3DB, UK."

Enhancement of the JET Edge LIDAR Thomson Scattering Diagnostic with Ultra Fast Detectors

M. Kempenaars¹, J.C. Flanagan¹, L. Giudicotti², M.J. Walsh¹, M. Beurskens¹,
I. Balboa¹ and JET EFDA contributors*

JET-EFDA, Culham Science Centre, OX14 3DB, Abingdon, UK

¹*EURATOM-UKAEA Fusion Association, Culham Science Centre, OX14 3DB, Abingdon, OXON, UK*

²*Consorzio RFX-Associazione Euratom-ENEA sulla Fusione, Corso Stati Uniti 4, I-35127, Padova, Italy*

** See annex of M.L. Watkins et al, "Overview of JET Results",
(Proc. 21st IAEA Fusion Energy Conference, Chengdu, China (2006)).*

Preprint of Paper to be submitted for publication in Proceedings of the
HTPD High Temperature Plasma Diagnostic 2008, Albuquerque, New Mexico.
(11th May 2008 - 15th May 2008)

ABSTRACT.

The edge LIDAR Thomson scattering diagnostic at the Joint European Torus fusion experiment uses a 3J ruby laser to measure the electron density and temperature profile at the plasma edge. The original system used a 1GHz digitizer and detectors with response times of $\approx 650\text{ps}$ and effective quantum efficiencies $< 7\%$. This system has recently been enhanced with the installation of a new 8GHz digitizer and four new ultra fast GaAsP microchannel plate photomultiplier tube detectors with response times of $< 300\text{ps}$ and effective quantum efficiencies in the range of $\sim 13\text{-}20\%$ (averaged over $\lambda = 500\text{-}700\text{nm}$). This upgrade has enabled the spatial resolution to be reduced to $\sim 6.3\text{cm}$ along the laser line of sight for a laser pulse of 300ps FWHM, which is close to the requirements for the ITER core LIDAR. Performance analysis shows that the new system will have an effective spatial resolution of up to 1cm in the magnetic mid-plane via magnetic flux surface mapping.

1. INTRODUCTION

The JET Tokamak is at present the largest fusion research facility in the world and is leading the way to the next step fusion machine ITER, it uses Light Detection and Ranging, LIDAR, Thomson scattering [1] for the measuring of the electron density and temperature in the plasma. This paper covers the upgrade of the edge LIDAR system on JET [2], with new ultra fast Gallium Arsenide Phosphide, GaAsP, microchannel plate photomultiplier tubes, MCP-PMTs, and will cover the detector response time, effective quantum efficiency, detector gating and switch-on and will show the first preliminary results. One of the key diagnostics at ITER will be the core LIDAR Thomson scattering system [3], the detector requirements for which are challenging and GaAsP detectors are one of the options.

2. THE JET EDGE LIDAR

The edge LIDAR system is designed to measure just the edge of the plasma at much higher effective spatial resolution than achievable along its line of sight, see figure 1 for a schematic of the optics layout of the edge LIDAR near the JET machine. The system's high spatial resolution is achieved by making the laser line of sight close to tangential to the plasma flux surfaces. The diagnostic was built in 1998 and partially upgraded in 2004 [4], but limitations in the detector availability and performance meant that this could not fully realise the systems potential. Due to this partial upgrade the JET edge LIDAR system used a combination of multi-alkali, MA-2, and GaAs MCP-PMTs, which have a measured response time $\tau_{\text{det}} \approx 650\text{ps}$ and $\tau_{\text{det}} \approx 500\text{ps}$ respectively, combined with a 1GHz (4GSa/s) digitiser, $\tau_{\text{dig}} \approx 350\text{ps}$. The ruby laser pulse length for the last operational period was measured to be as much as 1ns , although the initial specification for the laser was 330ps . The total system response before the present upgrade, assuming Gaussian responses for first order approximation, led to a spatial resolution of $\Delta_x \approx 12\text{cm}$, for 330ps laser pulse length and via the flux surface mapping this led to an effective spatial resolution of 2cm , depending on plasma configuration and laser alignment.

3. GaAsP MICROCHANNEL PLATE PHOTOMULTIPLIER TUBES

3.1 RESPONSE TIME

The goal was to replace the old detectors with 300ps response time detectors. The response times of the new detectors as quoted by the manufacturer were reproduced at JET, as shown in figure 2, compared

to the old detectors. It was found that the average response time of the detectors was approximately 290ps full width half maximum, FWHM. This response time was measured by illuminating the detector with a fast light pulser, in this case a sub 100ps pulsed light source at 650nm. On top of GaAsP being intrinsically faster than GaAs and MA-2, another design change that helps in achieving this faster response time is the size of the detector active area. On the old detectors this was 18mm, while on the new GaAsP detectors it is only 10mm diameter, which required a modification to the collection optics. The measurements confirm that the detectors are as fast as required for this upgrade and, although their active area is only 10mm, and have the added advantage of covering the whole spectrum on JET with a single detector type. Detectors with similar spectral and temporal bandwidth are needed for the ITER LIDAR [3]. The digitiser was replaced by a current technology digitiser, made possible by the advent of 20-40GS/s, 8 bit ADC technology, of course this speed needs to be matched by the signal cables connecting the detectors to the digitiser. This leads to a combined system response of $D_x = 6.3\text{cm}$, assuming a laser pulse width of $\sim 300\text{ps}$. According to our modelling this upgraded system is capable of achieving an effective spatial resolution of less than 1cm, via flux surface mapping.

3.2 EFFECTIVE QUANTUM EFFICIENCY

The effective quantum efficiency, EQE, of a detector is given by the photocathode quantum efficiency, QE, divided by the excess noise factor introduced by the microchannel plate:

$$EQE = \frac{QE}{NF^2} = \frac{[\langle S \rangle / \sigma]^2}{T \cdot \dot{N}}, \quad (1)$$

where T stands for the binning/integration time, \dot{N} is the number of input photons per nanosecond, $\langle S \rangle$ is the measured signal binned over period T and σ is the standard deviation on this signal over many repeats. So the QE is a measure of the photocathode alone, while the EQE incorporates the entire detector. Since these new detectors are faster than the old by about a factor 2, in order to maintain the signal to noise ratio it is necessary for their EQE to increase by at least a factor 2. The photocathode technology has over the last years dramatically improved as new materials have become available, see figure 3 for an overview of the effective quantum efficiency of the detectors used in the JET edge LIDAR system versus wavelength, including the new GaAsP detectors. The MA-2 detectors [5] have a QE of approximately 5.2% and an excess noise factor $NF^2 = 1.9$, which gives an EQE of 2.7%. The GaAs detectors have a measured QE of 26% however, their excess noise factor is high and the best detectors have an EQE of less than 6.5%. The new GaAsP detectors have an average QE of 24.5% while their excess noise factor is very low, the resulting EQE is in the range of $\sim 13\text{-}20\%$, averaged over $\lambda = 500\text{--}700\text{nm}$, with an average value of 17%, which is about a factor 3 higher than the detectors have had so far, this also shows that the signal to noise ratio will not only be preserved but should actually improve.

3.3 DETECTOR SWITCH-ON AND GAIN

A second requirement of the detectors is that they are gatable. This is because LIDAR is susceptible

to stray light from the laser and if the detectors are not gated at the right time the laser stray light will saturate the detector and ruin the measurements. Gating is achieved by applying a 250V pulse to the input of the microchannel plate, this gate on has to be completed in 5ns. The gate-on speed is clearly visible if a measurement of a DC light source is performed, as shown in figure 4. This figure also shows the old detectors and highlights the difference in signal to noise ratio. The gain of the detectors is a function of the voltage applied over the microchannel plate, in the order of 1700V, the gains achieved are in the order of $5 \cdot 10^6$.

4. RESULTS OBTAINED

This upgraded to the edge LIDAR system has been installed during a JET shutdown period in 2006 and has been running on JET since March 2008. Figure 5 shows the spectral function of the edge LIDAR system, the gap in channel 2 is for the H/D/T- α radiation. Results have been obtained, proving the viability of this system and its improved resolution. An example of raw data obtained with this new system is shown in figure 6. Note that since LIDAR is a time of flight technique, the horizontal axis can easily be translated from time to distance. The analysed data produced is along the laser line of sight, figure 7, this can then be mapped onto the machine midplane by use of flux surface mapping. Mapped data showing edge electron temperature and density and gradient measurements is depicted in figure 8, together with other JET diagnostics measuring the edge density and temperature profiles, showing the benefit from the LIDAR upgrade. This upgrade has also shown that a detector technology capable of achieving part of the ITER LIDAR requirement exists. However, these detectors have a good EQE for a wavelength range of 400-700nm, while the ITER system will need to cover 300-1200nm, more research in this field is required [6].

ACKNOWLEDGEMENTS

The authors would to thank the following people for their valuable contributions, without which this system would never have come to fruition; Don Simpson, Peter Heesterman, Adrian Capel, Roger Huxford, William Morris, Trevor Edlington, Frederic LeGuern and Armin Scherber. This work has been performed under the European Fusion Development Agreement. The views and opinions expressed herein do not necessarily reflect those of the European Commission.

REFERENCES

- [1]. H. Salzmann et al., The LIDAR Thomson Scattering Diagnostic on JET, JET-R(89)07 (EFDA-JET, Abingdon, U.K., 1989).
- [2]. C. Gowers, M. Beurskens, and P. Nielsen, *J. Plasma Fusion Res.* **76**, 874 (2000).
- [3]. M. Walsh et al., *Rev. Sci. Instrum.* **77**, 10E525 (2006).
- [4]. M. Kempenaars, et al., *Rev. Sci. Instrum.* **75**, 3894 (2004).
- [5]. ITT Electro-Optical Products Division, 1986, product No: F5-104A (F4128).
- [6]. L. Giudicotti, et al., 'Near-infrared detectors for ITER LIDAR Thomson scattering', 17th High Temperature Plasma Diagnostics Conference, May 2008, Albuquerque, USA.

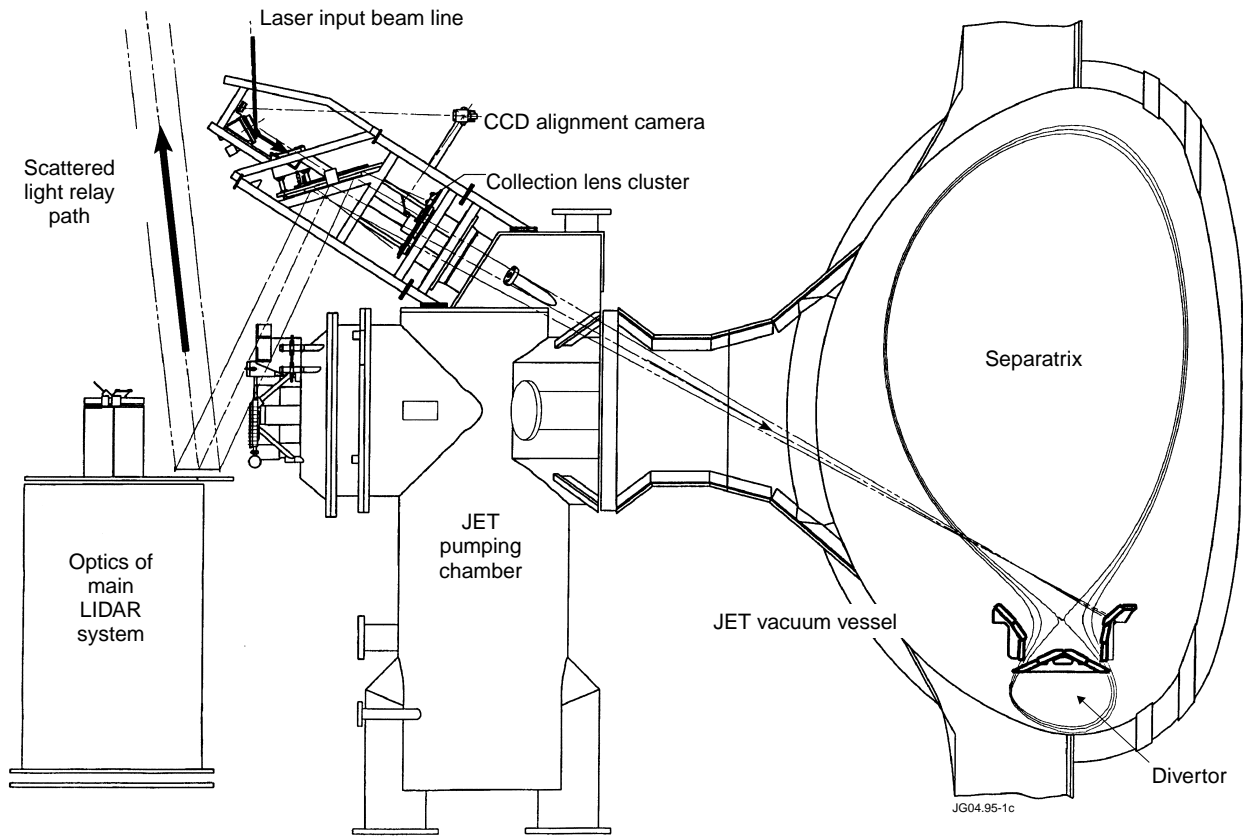


Figure 1: An overview of the JET edge LIDAR system optics near the Tokamak.

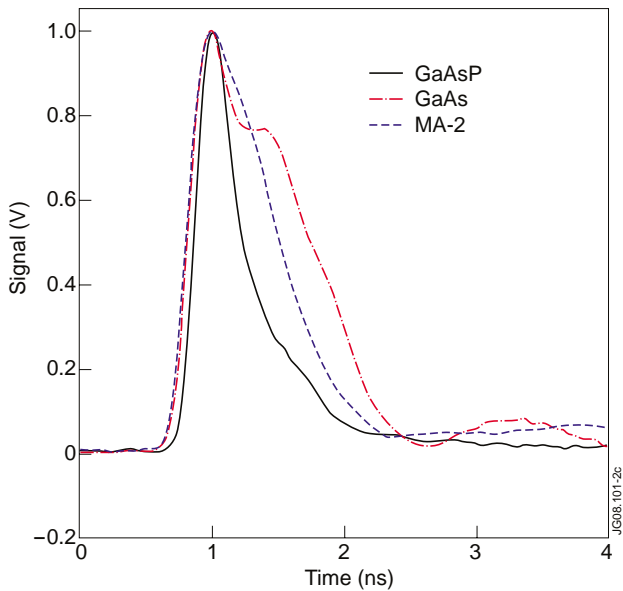


Figure 2: Detector response time as measured by the manufacturer and by the LIDAR team.

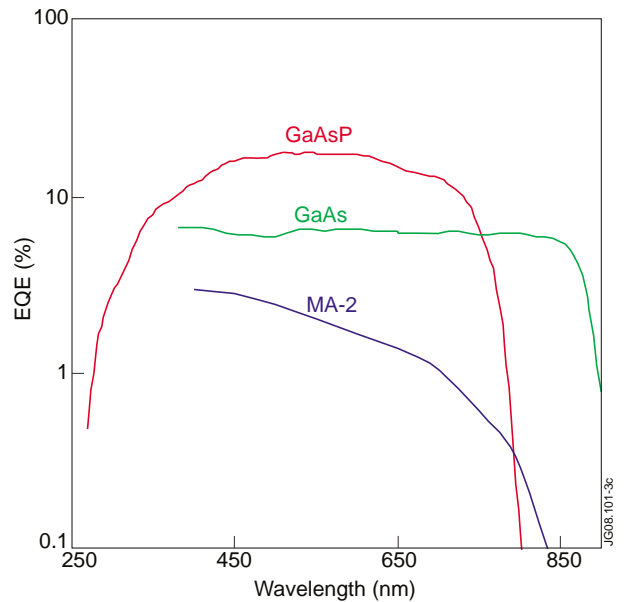


Figure 3: Effective quantum efficiency of the different detectors used on the JET edge LIDAR system; MA-2, GaAs and GaAsP. Note that the ruby laser wavelength is 694nm

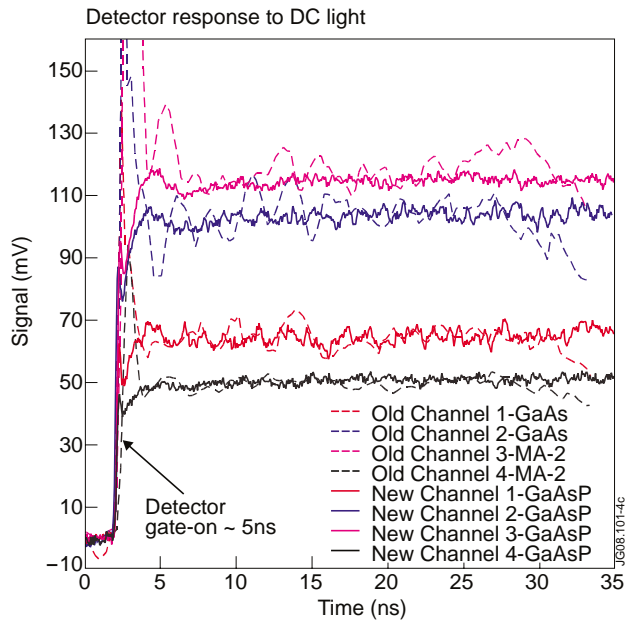


Figure 4: Detector responses to a DC light source, showing the comparison between the old and new detectors and the very fast switch-on $\sim 5\text{ns}$.

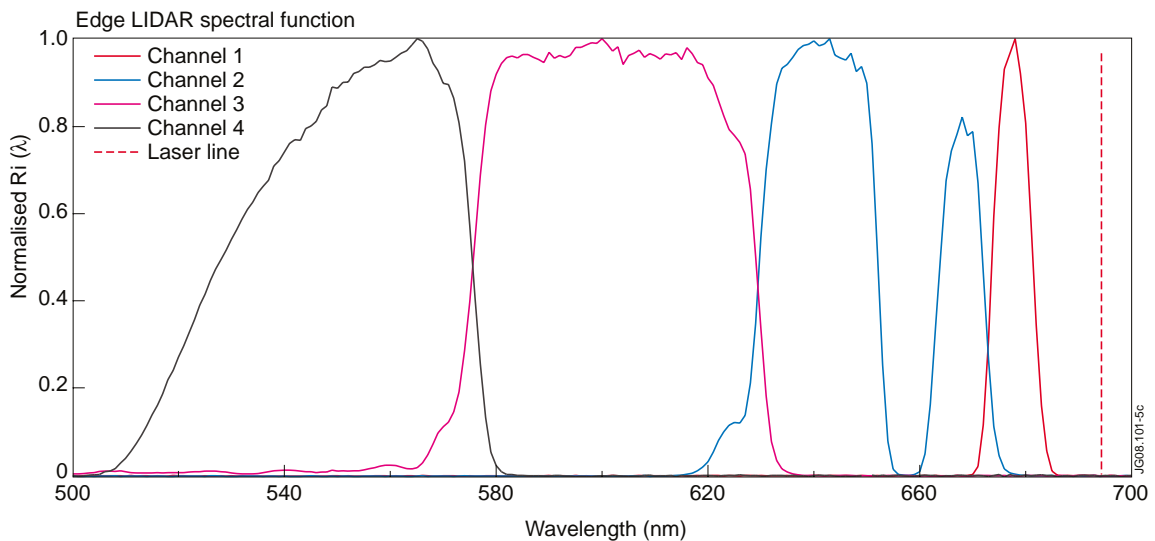


Figure 5: The edge LIDAR spectrometer spectral functions.

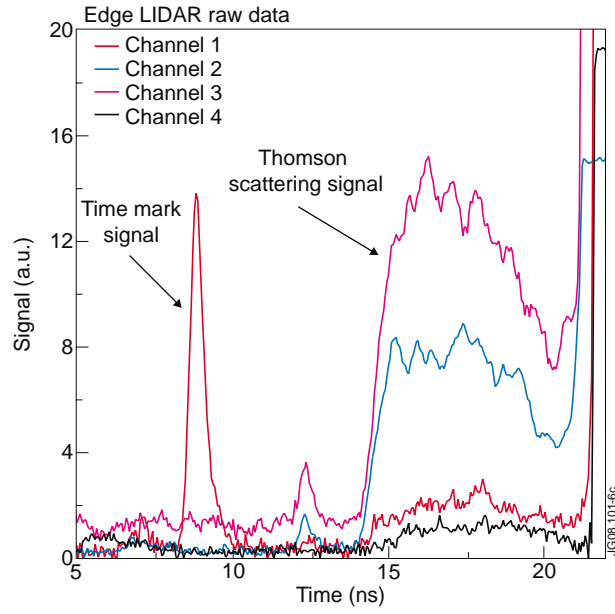


Figure 6: Raw data traces of the enhanced JET edge LIDAR system, showing the four detectors.

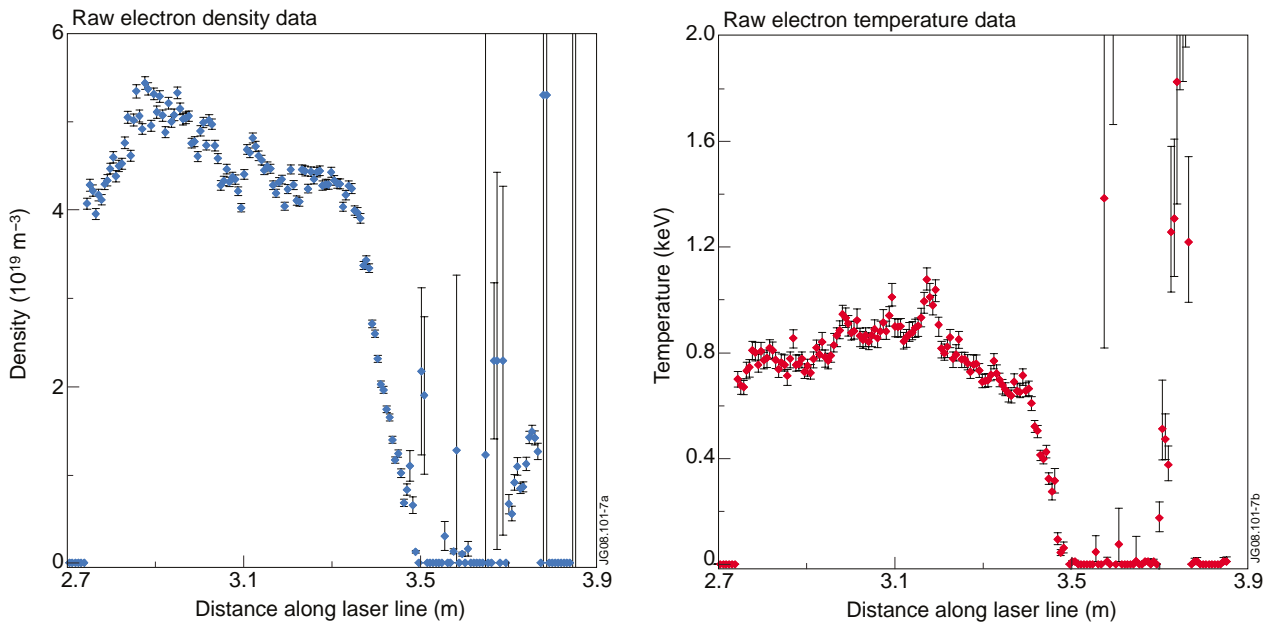


Figure 7: Data from the upgraded edge LIDAR system, showing the data along the laser line of sight.

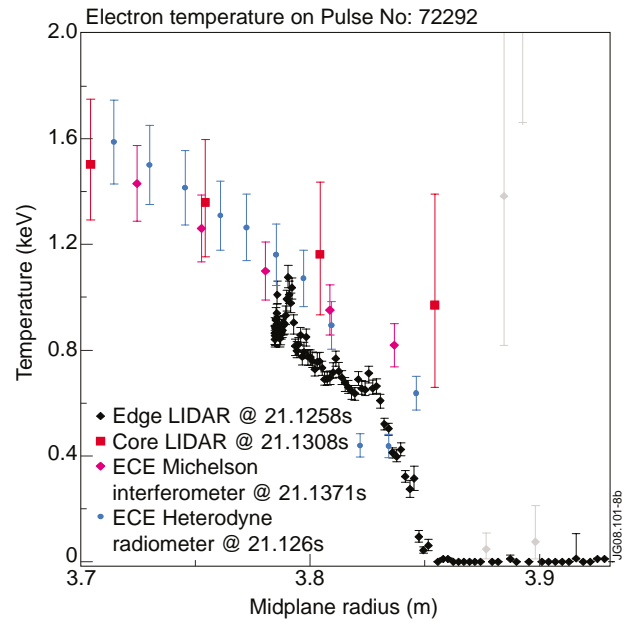
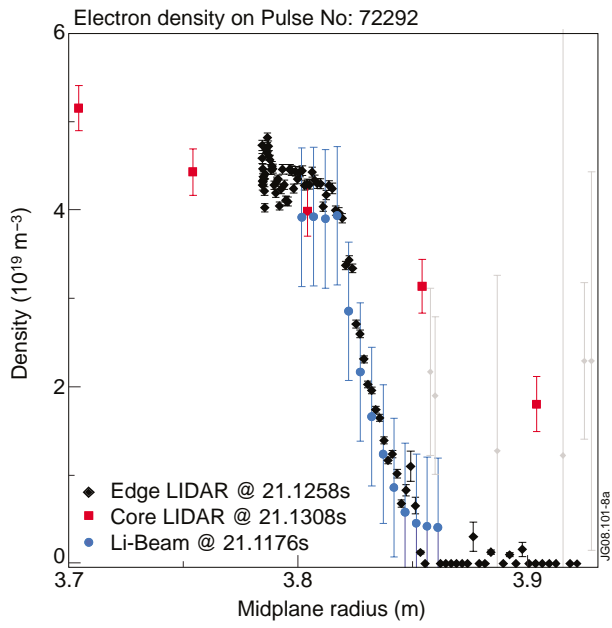


Figure 8: Showing the edge LIDAR data mapped on to the machine midplane and compared to other diagnostics